

## INFLUENCE OF ROTOR ANGLE INSTABILITY ON PROTECTION SYSTEMS IN DISTRIBUTION NETWORKS

Robert SCHMARANZ, Ignaz HÜBL  
KELAG Netz GmbH – Austria  
[robert.schmaranz@kelagnetz.at](mailto:robert.schmaranz@kelagnetz.at)  
[ignaz.huebl@kelagnetz.at](mailto:ignaz.huebl@kelagnetz.at)

Herwig RENNER  
Institute of Electrical Power Systems  
Graz University of Technology – Austria  
[herwig.renner@tugraz.at](mailto:herwig.renner@tugraz.at)

Michael MARKETZ  
KELAG – Austria  
[michael.marketz@kelag.at](mailto:michael.marketz@kelag.at)

### ABSTRACT

In this paper, a case study of a rotor angle instability in a distribution network is presented. The consequences for the grid operation are shown and the effects on protection devices are investigated. Further, the difference of the behavior of analogue and digital protection relays is discussed. Measurement and simulation results are compared and conclusions about the applicability of simplified models are presented. Finally, measures are presented to avoid similar situations in the future.

### INTRODUCTION

Rotor angle stability [1, 2, 3, 4] is a condition of equilibrium between opposing forces. The mechanism by which interconnected synchronous machines maintain synchronism is through restoring forces, which act whenever there are forces tending to accelerate or decelerate on one or more machines with respect to other machines. Under steady-state conditions, there is equilibrium between the input mechanical torque and the output electrical torque of each machine, and the speed remains constant. If the system is perturbed this equilibrium is upset, resulting in acceleration or deceleration of the rotors of the machines according to the mechanical equations of a rotating body. From the electrical point of view, this means rotating phasors of current and voltage related to the reference frame, which might have an influence on the behavior of protection devices [5, 6, 7].

These effects and the consequences on network operation are well-documented in high voltage transmission networks [8, 9, 10], but rarely at lower voltage levels. Therefore, this paper focuses on a case study, which took place in a 20-kV distribution network.

### TRANSIENT STABILITY

The case study deals with a transient instability of a synchronous generator feeding into a 20-kV network, as shown in Fig. 1.. Starting with a three-phase fault in feeder 3, the generator at busbar BB1 lost its transient angle stability and fell out of step. At the moment of the fault, the synchronous generator fed 11MW into the network.

During instability, both analogue distance protection relays at busbar BB3 in feeder 1 and 2 tripped. After that, the

circuit breaker in feeder 3 opened and cleared the fault.

The aim of this analysis is to study the protection behavior and the transient processes using the so called “simplified transient” or “classical” model. Additionally, the results should be checked and validated by means of an exact subtransient model. For further considerations, the power output and the excitation during the event are assumed to be constant. The results should be used to extend and/or change the protection concept of this area.

For the simplified configuration shown in Fig. 1., the relation between transferred power  $P_E$ , rotor angle  $\delta$  (related to the infinite bus) and maximum transferable power  $P_{\max}$  can be described as:

$$P_E = \frac{E' \cdot V_{BB4}}{X_T'} \cdot \sin(\delta) = P_{\max} \cdot \sin(\delta) \quad (1)$$

where  $E'$  is the transient internal voltage of the generator according to the current state of excitation,  $V_{BB4}$  the voltage at the infinite bus and  $X_T'$  the transient reactance between those voltages, including lines, transformers and machine parameters.

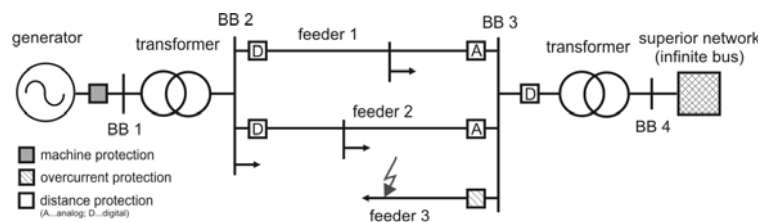


**Fig. 1.** Transient stability – grid scheme

The transient internal voltage-phasor of the generator can be calculated by:

$$\underline{E}' = \underline{E} - \sqrt{3} \cdot \underline{I}_{\text{prefault}} \cdot j(X_d - X_d') \quad (2)$$

with  $\underline{I}_{\text{prefault}}$  being the stationary prefault current-phasor,  $\underline{E}$  being the internal voltage-phasor according to the current state of excitation,  $X_d$  being the machine's synchronous reactance and  $X_d'$  being the transient impedance of the generator.

The maximum transferable power of the undisturbed grid (prefault, postfault) and during the fault can be seen in Table I. As the network consists mainly of short cable connections, the voltage drops during the fault to 2.8 kV.

**TABLE I**  
PARAMETER AND MAXIMUM POWER TRANSFER

	E	E'	V <sub>BB4</sub>	X <sub>T</sub>	P <sub>M</sub>	P <sub>max</sub>
	[kV]	[kV]	[kV]	[Ohm]	[MW]	[MW]
prefault, postfault	26.2	22.4	20.0	12.1	11.0	37.0
during fault	26.2	22.4	2.8	12.1	11.0	5.2

The power angle curves for this case are shown in Fig. 2. After fault clearing, a stationary point is extant, but it depends on the critical fault clearing time, if this operating point can be reached.

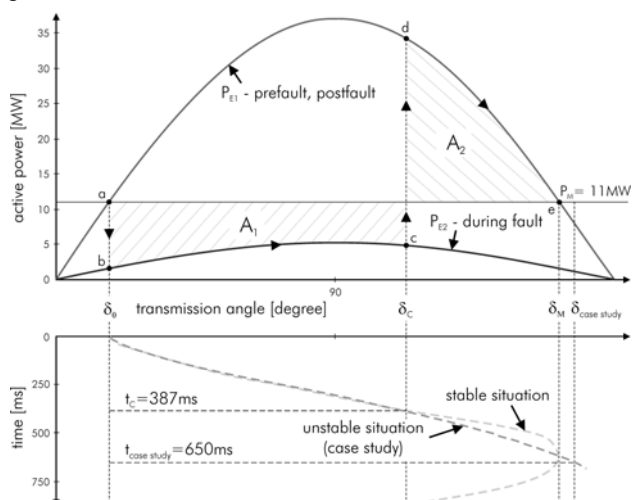


**Fig. 2.** Power-angle curve – transient stability

Initially, for a generation of 11MW, the operation point is at the angle  $\delta_0=17^\circ$  (point a). When the fault occurs, the operating point suddenly changes from a to b. Since the mechanical power is now greater than the electrical power, the rotor accelerates until the operating point reaches c, when the fault may be cleared. The operating point now suddenly changes at  $\delta_C$  to d. At this point, the electrical power is greater than the mechanical one, causing the rotor to decelerate. Since the rotor speed is greater than the synchronous speed, the angle  $\delta$  continues to increase until the kinetic energy gained during the period of acceleration (represented by the area  $A_1$ ) is expended by transferring the energy to the system. The operating point moves from d to e, such that area  $A_2$  is equal to area  $A_1$ .

The time-curve of the angle  $\delta$  for a stable situation and for the unstable situation (case study) can be seen in Fig. 2. The maximum angle to keep the system in a transient-stable state is at  $\delta_M=163^\circ$ . If this angle is not exceeded, the electrical power is still greater than the mechanical power and the rotor starts to retard. The rotor angle decreases, and the operating point retraces the path from e to d and follows the postfault curve farther down. The minimum value of  $\delta$  is such that it satisfies the equal-area criterion for the postfault system. Depending on the damping, the system oscillates around the equilibrium point a, where it finally settles in. The critical clearing angle  $\delta_C$  for this case can be obtained graphically using the equal-area criterion ( $A_1=A_2$ ):

$$A_1 = \int_{\delta_0}^{\delta_C} P_M - P_{E2}(\delta) d\delta \quad (3)$$

$$A_2 = \int_{\delta_C}^{\delta_M} P_{E1}(\delta) - P_M d\delta \quad (4)$$

This leads to an critical clearing angle of  $\delta_C = 113^\circ$ .

With the maximum angle excursion  $\delta_C$  and the total inertia moment J of the generator and turbine, the critical clearing time  $t_C$  can be calculated with [4]:

$$H = \frac{\omega_n^2 \cdot J^2}{2 \cdot p^2 \cdot S_N} \quad (5)$$

$$t_C = \sqrt{4 \cdot \frac{H}{\omega_n} \cdot \frac{S_N}{P_A} (\delta_C - \delta_0)} \quad (6)$$

where H is the normalized inertia constant of generator and turbine and  $P_A$  is the average accelerating active power. Damping torques by the machine's damper winding are neglected in this simplified calculation. The results of these calculations can be found in Table II.

**TABLE II**  
MAXIMUM ANGLE AND DELAY-TIME

	$\delta_0$	$\delta_M$	$\delta_C$	H	$t_C$
	[°]	[°]	[°]	[sec]	[ms]
transient stability case	17	163	113	3.0	387

To keep the system transient stable, the maximum angle  $\delta_C$  is not allowed to exceed  $113^\circ$ . Thus, the duration of this fault has to be shorter than 387 ms.

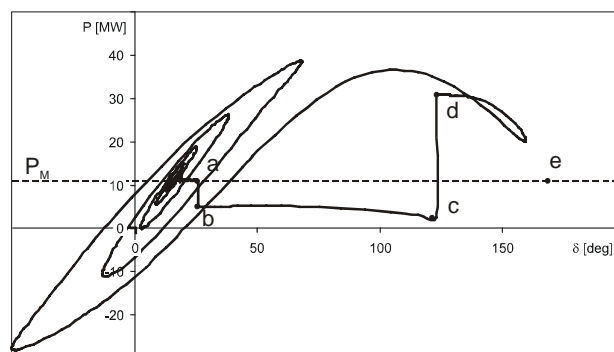


**Fig. 3.** Power versus angle curve for subtransient model with voltage regulation system and critical fault clearing time of 410 ms

A complex simulation subtransient model, taking into account the effect of damping and action of the voltage regulation systems leads to a critical fault clearing time of 410 ms. Fig. 3. shows the corresponding P- $\delta$ -curve. For further considerations, the results of the simplified transient model are used. With the simplifications there is a safety margin in the results, which is necessary considering uncertainties in the base data.

### BEHAVIOR OF PROTECTION RELAYS

The fault in the case study was a three-phase fault cleared by the protection relay in feeder 3 after 1.2 seconds. The analogue protection relays at busbar BB3 in feeder 1 and 2 tripped after 650 ms. In that time, the generator lost synchronism.

The electrical voltages and currents during instability are generally three-phase symmetrical. At busbar BB1, the infeed of the generator, the voltages as well as the currents shifted away. On the other side at busbar BB3, the voltages were, stabilized by the voltage of the infinite bus, constant in their phase position.

The current phasors of feeder 1 as well as the constant voltage phasor of the infinite bus can be seen in Fig. 4. The diagram shows the vectors from the beginning of the fault until line-tripping of feeder 1. The phase currents shifted within 650 ms by 150° as a consequence of the instability of the generator. The voltages at busbar BB1 were rotating in the same way.

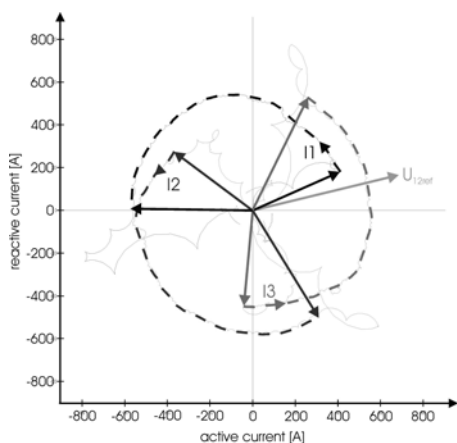


**Fig. 4.** Current diagram of feeder 1 and reference voltage phasor

During this event, the same behavior of protection relays could be observed for different protection relay generations: The two analogue distance protection relays at busbar BB3 in feeder 1 and 2 were tripping in forward direction. At first sight, the behavior of these relays seemed to be incorrect, but detailed analysis resulted in the following explanation. The protection relays in these feeders were measuring a small, but constant voltage without any vector rotation. The currents in these feeders were rotating, supplied by the unstable generator. When the vector-shift between voltage and current at BB3 became larger than 90°, the direction recognition of the protection devices switched from “backward” to “forward”. The direction “forward” results in a shorter tripping time and both relays cleared an apparently close, forward fault.

The digital protection relays in feeder 1 and 2 at busbar BB2 correctly recognized the fault in the first time as “forward”. After a current phase-shift of 110°, the direction for these relays changed to “backwards”. This behavior can be explained by the characteristic of this digital protection

relay type.

Within the first 40 ms, the algorithm of this protection relay uses stored voltages for the general reference of any direction evaluation. Afterwards, the relay still uses the stored voltages, if the measured voltage is smaller 40% of the nominal voltage  $U_N$ . An update of the voltage-storage occurs as long as no pickup and no sudden change in the measures signals occur. This voltage is available for a maximum time of 5 seconds. If there is no corresponding stored voltage available, another voltage (e.g.  $V_{12}$  instead of  $V_{23}$ ) is used, which also has to be higher 40% of  $U_N$ .

For the distance protection relays at busbar BB2, the voltage dropped at the beginning of the fault to values smaller 20% of  $U_N$ . Therefore, the stored (prefault) and constant voltage was used for direction evaluation and the angle between the stored voltage and the rotating current increased steadily. At an angle higher 90°, the direction calculation changed from “forward” to “backward”.

This change in direction didn't have any effect on the power system, as these relays didn't trip. However, this characteristic is not described in the user manuals. For protection engineers, it is important to know the behavior of the direction evaluation during unstable situations.

### PROTECTION-RELATED MEASURES

In the future, an unstable generator in this network must not influence the selectivity of the protection devices. Therefore, a further calculation was done considering the worst case scenario. The result of this calculation will be implemented into the protection concept.

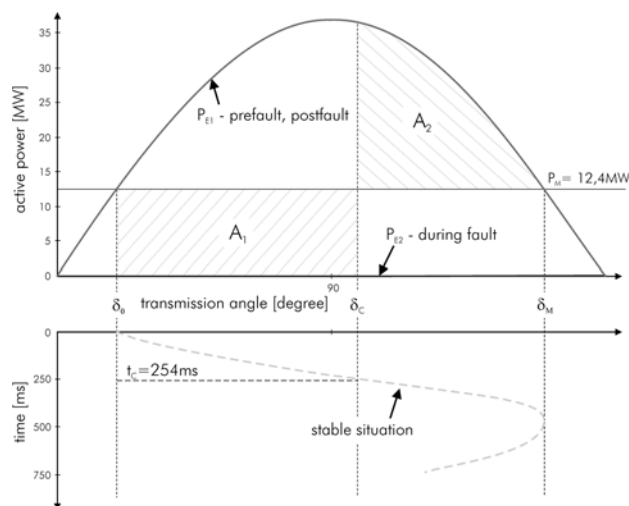


**Fig. 5.** Power angle curve „worst case“

For the calculation of stability limits, the nominal values of the generator ( $S_N, \cos\phi_N$ ) have to be assumed as operational parameters [4]. For any lower generation, the maximum allowed fault duration will be longer and therefore not as critical. The second assumption for the worst case scenario is, that the maximum power transmission during the fault is zero, which results in a maximum acceleration of the rotor. The power angle curve under these assumptions and the

calculated results can be seen in Fig. 5. and Table III. The critical clearing angle  $\delta_c=97^\circ$  is equivalent to a time of  $t_c=254$  ms. This time is the maximum allowed duration for any fault in this grid to avoid transient instability and non-selective protection relay tripping.

**TABLE III**  
TRANSIENT STABILITY „WORST CASE“

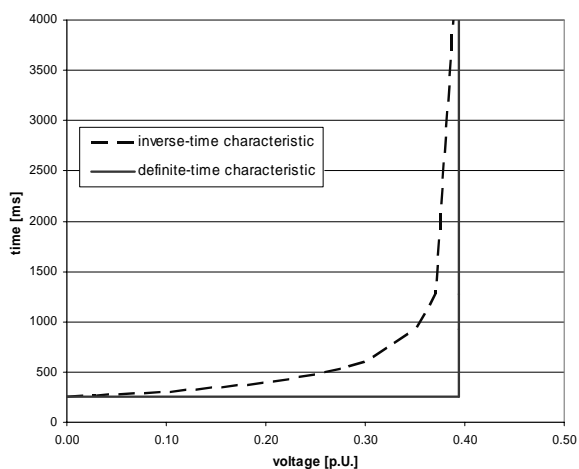
	E	E'	V <sub>BB4</sub>	X <sub>T</sub>	P <sub>M</sub>	P <sub>max</sub>
	[kV]	[kV]	[kV]	[Ohm]	[MW]	[MW]
prefault, postfault	26.2	22.4	20.0	12.1	12.4	37.0
during fault	26.2	22.4	0.0	12.1	12.4	0.0

	$\delta_0$	$\delta_M$	$\delta_C$	H	t <sub>C</sub>
	[°]	[°]	[°]	[sec]	[ms]
transient stability case	20	160	97	3.0	254

Different fault locations and fault impedances result in different voltage sags and therefore in different transferable power values during the fault. The voltage during a fault is the major factor for the stability limit. Thus, this voltage has to be varied to obtain a tripping characteristic for different events in the network.

The inverse-time tripping characteristic (Fig. 6.) shows the maximum allowed fault duration depending on different voltage sags. If the voltage doesn't drop below 0.40 p.u., no instability will occur and no voltage-dependent tripping must be executed.



**Fig. 6.** Voltage-time diagram for protection setting

A further and simpler tripping characteristic is the definite-time stage characteristic. If no inverse-time tripping can be realized, the relay can be set to the simplified definite-time characteristic shown in Fig. 6. In this curve, every voltage sag below 0.40 p.u. leads to a protection tripping after 250 ms. This curve is easier to implement but gives no time-flexibility for the protection devices.

Due to the staggering of the different protection relays, the grid protection can not guarantee a maximum clearing time of 250 ms. Therefore, these curves have to be applied to the machine protection. With these measures, the generator will be disconnected before instability occurs, and non-selective and unwanted protection tripping will be avoided.

## CONCLUSION

Rotor angle stability is well-documented in transmission networks but rarely at other voltage levels. In this paper, an event in a distribution system is presented and a rotor angle instability is identified. Further, the steps for analyzing such an event are shown. The results from measurements are compared with simulations of different complexity. Calculations with simplified models provide more conservative results. Furthermore, the consequences on the network protection are discussed and solutions are presented. These discussions have to go on with manufacturers of protection devices to develop further solutions for unstable network situations.

## REFERENCES

- [1] P. Kundur, 1994, *Power System Stability and Control*, EPRI Power System Engineering Series, McGraw-Hill Inc., New York, USA
- [2] H. Renner, 2004, *Netzregelung und -stabilität*, Vorlesungsunterlagen, Technische Universität Graz, Institut für Elektrische Anlagen, Graz, Austria
- [3] R. Muckenhuber, 1985, *Elektrische Energieübertragung*, Technische Universität Graz, Institut für Elektrische Anlagen, Graz, Austria
- [4] H. Happoldt, D. Oeding, 1987, *Elektrische Kraftwerke und Netze*, Fünfte Auflage, Springer Verlag, Austria
- [5] ALSTOM, 2002, *Network Protection and Automation Guide*, Energy Automation & Information, France
- [6] H. Hubensteiner, 1993, *Schutztechnik in elektrischen Netzen 2*, Technische Akademie Esslingen, VDE-Verlag GmbH, Berlin, Germany
- [7] R. Grondin, A. Heniche, M. Dobrescu, G. Trudel, M. Rousseau, B. Kirby, S. Richards, A. Apostolov, 2006, "Loss of Synchronism Detection, a Strategic Function for Power System Protection", *CIGRE Conference*, Publication No. B5-205, Paris
- [8] D.Z. Meng, 2006, "Maintaining System Integrity to Prevent Cascading Blackout", *CIGRE Conference*, Publication No. B5-207, Paris
- [9] S. Gal, F. Balasiu, M. Cernat, A. Popescu, M. Petran, 2006, "Defence Plan against Major Disturbances in the Romanian Power Grid", *CIGRE Conference*, Publication No. B5-212, Paris
- [10] J. Tsukida, H. Kameda, T. Yoshizumi, T. Matsushima, Y. Kawasaki, M. Usui, 2006, "Experiences and Evolution of Special Protection Systems in Japan", *CIGRE Conference*, Publication No. B5-209, Paris